

## Mineralogical studies and extraction of some valuable elements from sulfide deposits of Abu Gurdi area, South Eastern Desert, Egypt

Ibrahim A. Salem<sup>1</sup>, Gaafar A. El Bahariya<sup>1</sup>, Bothina T. El Dosuky<sup>1</sup>, Eman F. Refaey<sup>1</sup>,  
Ahmed H. Ibrahim<sup>2</sup>, and Amr B. ElDeeb<sup>2</sup>★

<sup>1</sup>Geology Department, Faculty of Science, Tanta University, Tanta, Egypt

<sup>2</sup>Mining and Petroleum Department, Faculty of Engineering, Al-Azhar University, Nasr City, Cairo 11884, Egypt

(Received September 17, 2023; Revised November 20, 2023; Accepted November 20, 2023)

**Abstract:** Abu Gurdi area is located in the South-eastern Desert of Egypt which considered as volcanic massive sulfide deposits (VMS). The present work aims at investigating the ore mineralogy of Abu Gurdi region in addition to the effectiveness of the hydrometallurgical route for processing these ores using alkaline leaching for the extraction of Zn, Cu, and Pb in the presence of hydrogen peroxide, has been investigated. The factors affecting the efficiency of the alkaline leaching of the used ore including the reagent composition, reagent concentration, leaching temperature, leaching time, and Solid /Liquid ratio, have been investigated. It was noted that the sulfide mineralization consists mainly of chalcopyrite, sphalerite, pyrite, galena and bornite. Gold is detected as rare, disseminated crystals within the gangue minerals. Under supergene conditions, secondary copper minerals (covellite, malachite, chrysocolla and atacamite) were formed. The maximum dissolution efficiencies of Cu, Zn, and Pb at the optimum leaching conditions i.e., 250 g/L NaCO<sub>3</sub> - NaHCO<sub>3</sub> alkali concentration, for 3 hr., at 250 °C, and 1/5 Solid/liquid (S/L) ratio, were 99.48 %, 96.70 % and 99.11 %, respectively. An apparent activation energy for Zn, Cu and Pb dissolution were 21.599, 21.779 and 23.761 kJ.mol<sup>-1</sup>, respectively, which were between those of a typical diffusion-controlled process and a chemical reaction-controlled process. Hence, the diffusion of the solid product layer contributed more than the chemical reaction to control the rate of the leaching process. High pure Cu(OH)<sub>2</sub>, Pb(OH)<sub>2</sub>, and ZnCl<sub>2</sub> were obtained from the finally obtained leach liquor at the optimum leaching conditions by precipitation at different pH. Finally, highly pure Au metal was separated from the mineralized massive sulfide via using adsorption method.

**Key words:** complex sulphide ores, extractive metallurgy, hydrometallurgy, alkaline leaching; kinetic

### 1. Introduction

Recently, attention has been drawn to low-grade complex sulphide ores due to the decline in the world deposits of high-grade ores. Complex sulphide

ores are in many cases difficult to treat with conventional mineral processing methods and the concentrates produced are often not clean enough, which seriously limits their commercial value.<sup>1</sup>

Currently, copper is considered one of the base

★ Corresponding author

E-mail : dr.basuony2016@azhar.edu.eg

This is an open access article distributed under the terms of the Creative Commons Attribution Non-Commercial License (<http://creativecommons.org/licenses/by-nc/3.0>) which permits unrestricted non-commercial use, distribution, and reproduction in any medium, provided the original work is properly cited.

metals which has high economic importance in advanced technologies. About 80 % of the primary copper production comes from pyrometallurgical treatment of copper ores.<sup>2,3</sup>

Recently, the economic conditions and the increasingly stringent environmental legislation worldwide have led to restricting the progress of the metallurgical industries. In addition, copper resources become increasingly depleted, and the number of low-grade refractory copper ore is continuously increasing. Therefore, more attention must be paid to developing cost-effective, eco-friendly processes of recovering copper from low-grade ores. The extraction of copper from their ores is commonly performed using mainly pyrometallurgical, hydrometallurgical and bio-chemical, in which the extraction equipments always suffered from serious erosion and corrosion problems leading to high production cost.<sup>4,5</sup>

Recently, the depletion of high-grade copper oxide ores in addition to the presence of toxic elements in concentrates such as carcinogenic arsenic and due to the increasing relevance of ESG (Environmental, Social & Governance) regulation risk management, the hydrometallurgical option for processing flotation concentrates has become more attractive, because it represents an eco-friendly process compared to pyrometallurgical processes.<sup>6,7</sup> In this aspect, developing advanced leaching technologies for processing copper sulfide ores using hydrometallurgical techniques, has been intensified.<sup>8-12</sup>

Copper ores can be considered as classical examples which are treated by hydrometallurgical processes. Generally, either copper oxides or roasted copper sulfides are leached without requiring any further oxidation.<sup>13,14</sup> Sulfuric acid ( $H_2SO_4$ ) and ammonia ( $NH_3 \cdot H_2O$ ) are usually used as lixiviant in the leaching copper ores, such as chalcocite ( $Cu_2S$ ), malachite [ $Cu_2(CO_3)(OH)_2$ ]. Sulfuric acid is the most common leaching reagent used for the dissolution of oxidized copper ores because copper oxide ore can be dissolved in  $H_2SO_4$  solution even at room temperature. Thus, the sulfuric acid consumption dosage is the main economic factor in the leaching process. Depending on the characteristic of the ores, sulfuric acid consumption

could range from 0.4 to 0.7 Mg for each Mg of copper recovered.<sup>15</sup> However, energy consumption can also become an important economical factor when the leaching process runs under the condition of agitation and heating. Studying the kinetics of copper leaching is therefore necessary for determining the factors that affect the leaching efficiency.

The kinetics of copper leaching has been investigated in many previous works.<sup>16-19</sup> The kinetics of copper leaching from a chalcocite-covellite ore has been investigated and the rate-determining steps for each period were determined according to both the activation energies and the analytical expressions for each period.<sup>16</sup> The dissolution kinetics of malachite during the leaching was described by a logarithmic function,  $y = a \ln(x) + b$  and it was noted that the initial dissolution of malachite was a diffusion-controlled reaction.<sup>17</sup> The dissolution kinetics of  $CuO/Al_2O_3$  catalyst in inorganic acid solutions has been studied.<sup>18</sup> It has been noted that the rate of malachite dissolution could be modeled in two stages. The first stage was a diffusion-controlled reaction and the dissolution for the second stage was a chemical-controlled reaction.<sup>19</sup> However, few researches were carried out on the hydrometallurgical processing of low-grade cuprite-type copper oxide ore. This kind of ore is usually processed by milling then froth floating, but the recovery of copper is lower than 50 % using this technology based on the previous studies.<sup>20</sup> For the foregoing reason, further research is still needed for effective exploitation of this kind of ore.

The leaching of copper depends on effective liberation of sulphide ore from gangue minerals, which includes carbonates of magnesium, calcium and other metals. The presence of such carbonates results in parallel reactions taking place simultaneously and hence introduces competition in the system for the acid reagent.<sup>21,22</sup> The shrinking core model has been used elsewhere to evaluate the kinetics of leaching process since the ground particles are assumed to be spherical.<sup>23,24</sup>

Abu Gurdi area is located at 60 km from Baranis, South-eastern Desert, Egypt. It is delineated by latitudes  $23^{\circ}45'$  and  $24^{\circ}05' N$  and longitudes  $34^{\circ}59'$

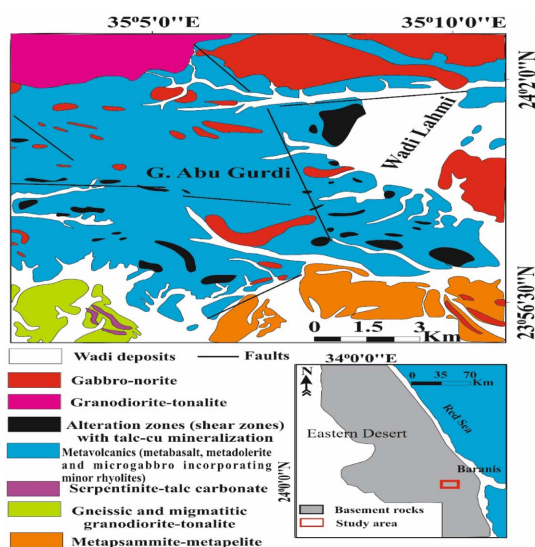


Fig. 1. Detailed geological map of Abu Gurdi area (modified after EGSMA, 1992).<sup>31</sup>

and 35° 10'E as shown in Fig. 1. The volcanic massive sulfide deposits (VMS) of Abu Gurdi are associated with metavolcanic rocks. The Geology of Abu Gurdi area has extensively been studied in many previous studies. The sulphide mineralization was found essentially in the form of small lensoid and veins of 3 m wide and 20 m long.<sup>25-29</sup>

Zinc, Lead, and Copper are also widely used metals in the different industrial applications. They are mainly produced from sulfides, carbonates and partly from various secondaries and wastes containing zinc such as electric arc furnace dusts, zinc ash, zinc dross, scraps, slags by hydrometallurgical, pyrometallurgical or their combination processes.<sup>30</sup>

Many efforts were carried out to develop the hydrometallurgical method for increasing the percent recovery of Zn, Cu and Pb. Inorganic acids have been commonly used as leach reagent in these studies.<sup>32-35</sup> In addition to this, organic acids have also been applied as leach reagents in recent years.<sup>36-39</sup> More attention has been focused on the alkaline treatment of low-grade zinc oxide ores.<sup>40-45</sup> In the hydrometallurgical processes, different alkaline lixiviants can be used including NaOH, NH<sub>4</sub>OH, NH<sub>4</sub>(CO<sub>3</sub>) and NH<sub>4</sub>(Cl).<sup>30,44,46-50</sup>

Alkaline leaching has many advantages including

selectivity, cost-effectiveness, simple and easy to operate and managed to extract metal ions from oxidized ores or wastes.<sup>40-42</sup> It was concluded that the maximum recovery of about 89 % and 72.15 % of Zn and Pb, respectively has been obtained at temperature 80 °C, 4 M NaOH, 20 ml/g L/S ratio and 500 rpm agitation speed of for lead leaching and 400 rpm for zinc dissolution.<sup>51</sup>

The present work aims to investigate the ore mineralogy in Abu Gurdi region and investigates the effectiveness of a hydrometallurgical route for processing these ores using Alkaline leaching for the extraction of zinc, copper, and lead in the presence of hydrogen peroxide. The optimization of the leaching conditions for recovery of high purity Copper, Zinc, Lead and precious gold and the factors affecting the leaching process have been investigated. The kinetics of the leaching process has also been studied.

## 2. Materials and Methods

### 2.1. Materials

The as received 10 kg of the volcanic massive sulphide deposits (VMS) sample was collected from Abu Gurdi mining site, which is located 60 km from Baranis, South-eastern Desert, Egypt, that is delineated by latitudes 23°45' and 24° 05' N and longitudes 34° 59' and 35° 10'E. Leaching reagents of chemically pure grade including NH<sub>4</sub>OH, Na<sub>2</sub>CO<sub>3</sub>, NaHCO<sub>3</sub>, (NH<sub>4</sub>)<sub>2</sub>CO<sub>3</sub>, NH<sub>4</sub>HCO<sub>3</sub>, (NH<sub>4</sub>)HCO<sub>3</sub> have been used during the leaching process and were purchased from El-Nasr Company for Intermediate Chemicals, El-Giza governorate, Egypt.

### 2.2. Methods

#### 2.2.1. Mineralogical study

The main mineral constituents of the used Abu Gurdi deposits have been identified in order to obtain detailed mineralogical study. The rock sample was first ground and then sieved into the size -63 μm. The light and heavy fraction were separated using bromoform (sp. gr. 2.8 gm/cm<sup>3</sup>, Merk- Germany). The heavy mineral particles were picked under a binocular microscope (Optech, LFZT - Germany) and

identified by Scanning Electron Microscope (SEM) a Philips Model XL 30 supported by an energy dispersive X-ray unit (EDS) for semi-quantitative analysis.

### 2.2.2. Sample characterisation

A representative sample of the technological sample that had been collected adequately prepared for a comprehensive chemical and mineralogical analysis in addition to the tenor of the economic metal values that had been collected. The main oxides were determined by XRF using a sequential XRF spectrometer (XRF-1800, 40 kV, 90 mA, Re anode, Shimadzu, USA). Also, Scanning Electron Microscope (SEM-EXL 30 Philips type) coupled with X-ray analyzer (EDS unit system) was utilized as a guiding semi-quantitative analysis of the purity of obtained final products.

### 2.2.3. Leaching process

The dissolving efficiency of Zn, Cu and Pb was investigated by using the alkaline agitation leaching technique under a variety of various settings. In each experiment, a constant weight of the crushed ore sample fraction (10 g) was combined with an alkaline solution of known concentration at a specific S/L ratio. The pulp was agitated for a predetermined time at a predetermined temperature before being discarded. After the finishing of each leaching experiment, the obtained slurry was then filtered and washed with hot distilled water to remove any liberated metal ions during the leaching process. The obtained pregnant and washing solutions were then combined to make up the total volume of the leaching solution. Appropriate aliquots of the produced leaching solution were then analysed for the content of Zn, Cu and Pb that had been leached in order to calculate their respective leaching efficiencies. Moreover, leaching or dissolution efficiency of Cu, Zn and Pb metal ions was calculated according to Eq. (1).<sup>36,37</sup>

$$R(\text{Zn, Cu, Pb}) = \left( \frac{m_1 \cdot v_1}{m_0 \cdot v_0} \right) * 100 \quad (1)$$

Where  $m_0$  and  $m_1$  are the mass of ore used in leaching experiments (g) and the concentration of

metal ions (Zn, Cu and Pb) in the filtrate (g/L), respectively.  $v_0$  and  $v_1$  are the mass percentage of metal ions (Zn, Cu and Pb) in ore (%) and the volume of filtrate (L), respectively.

The factors affecting the leaching process include the reagent composition, the alkali concentration, leaching time, leaching temperature, solid/liquid ratio have been investigated. Studying these factors would result in the proper selection of the optimum conditions considering the efficiency of the leaching process and economic considerations.

### 2.2.4. Recovery of high purity metal ions

Using alkaline compounds in leaching process of the studied ore have many advantages including obtaining highly pure Zn, Cu and Pb concentrates, and at the same time prevent iron dissolution and the formation of silica gel. These concentrates were recovered from the leaching solution by the precipitation procedures firstly as bulk hydroxides precipitate at pH 7-8. Then, the mixed precipitate is subjected to relatively severe treatment with  $\text{H}_2\text{SO}_4$  to selectively separate the interested metal value Cu followed by separating Zn and Pb using conventional techniques.

## 3. Results and Discussion

### 3.1. Comprehensive characterization of sulfide mineralization

#### 3.1.1. Mineralogical investigation

Ore microscopic observations and scanning electron microscope (SEM) were used to identify the different ore and gangue minerals. The obtained results of scanning electron microscope examination support the results of reflected light microscope study. The following is a brief account of the main microscopic features of these minerals:

Chalcopyrite is the most common sulfide mineral, commonly accompanied by sphalerite and pyrite. It occurs as coarse subidiomorphic to xenomorphic crystals (0.5-1.2 mm) with dark yellow colour with weak anisotropism as shown in *Fig. 2A*. Occasionally, some chalcopyrite crystals are partially altered to covellite along the periphery, forming rim replacement.

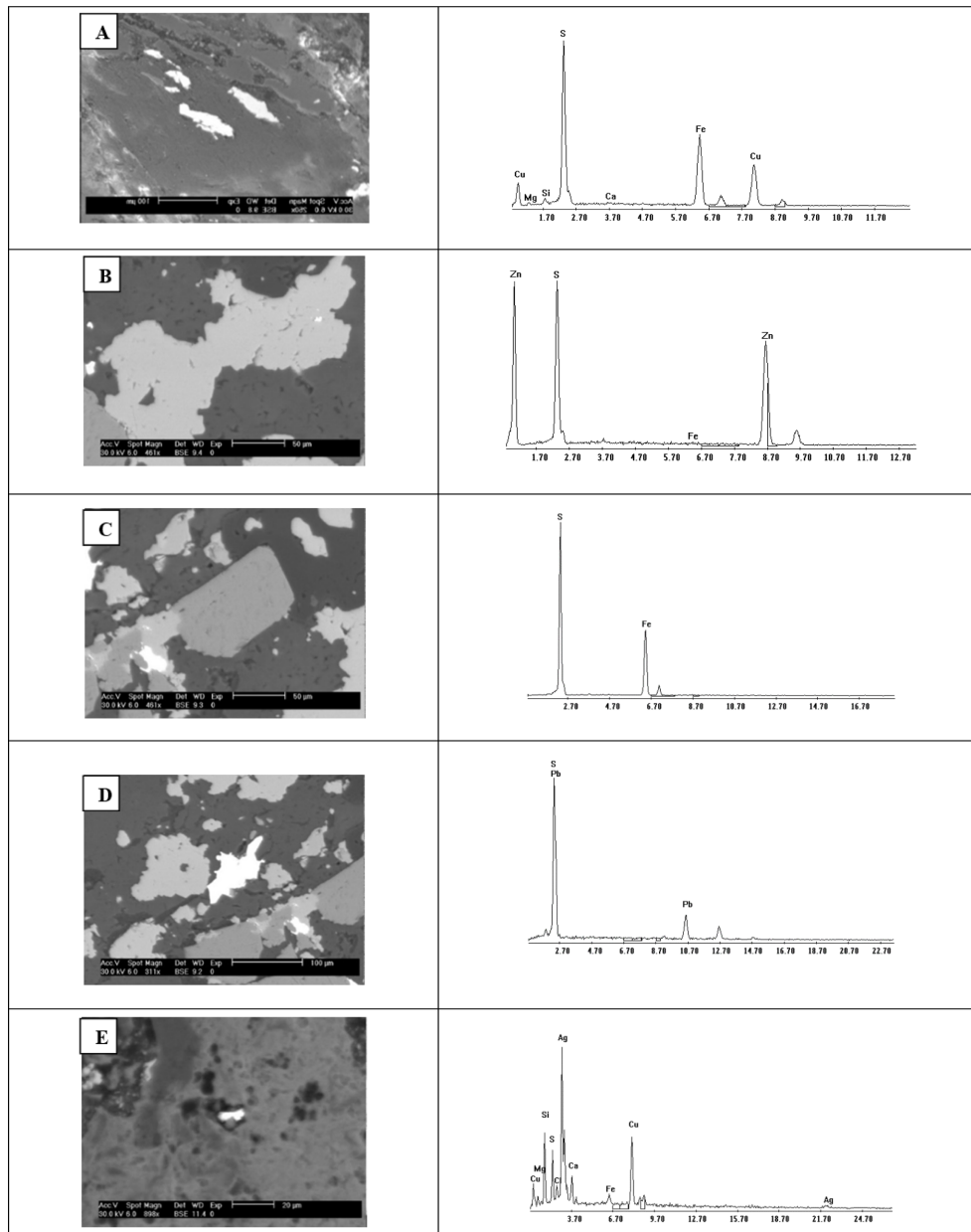


Fig. 2. SEM image and EDX analysis data of A) Chalcopyrite, B) Sphalerite, C) Pyrite, D) Galena and E) Jalpaite minerals.

Sphalerite occurs in considerable amounts next to chalcopyrite as coarse subidiomorphic to xenomorphic crystals (0.3-1.5 mm) of grey colour as shown in Fig. 2B. It usually contains rounded to subrounded chalcopyrite blebs forming emulsion solid solution at temperature above 350 °C.<sup>52</sup> Pyrite occurs as fine to medium idiomorphic to subidiomorphic crystals

(0.01-0.2 mm) of creamy white color and high reflectivity as shown in Fig. 2C. Pyrite grains are fractured and fragmented. It is commonly accompanied by chalcopyrite, sphalerite and galena. Galena occurs in small amount as granular subidiomorphic crystal of light grey colour, characterized by visible cleavage and triangular pits as shown in Fig. 2D. Fine grains

of pyrite are observed scattered in galena. Bornite has pinkish brown colour and is mostly found as granular aggregates (0.01-0.6 mm). Exsolved lamella of chalcopyrite are observed within the bornite grains. Chalcopyrite and bornite form a solid solution at a temperature above 475 °C.<sup>53</sup> Jalpaite ( $3\text{Ag}_2\text{S}\cdot\text{Cu}_2\text{S}$ ) is a type of silver group minerals, occurs as fine discrete

grains with detectable silver content (*Fig. 2E*).

Secondary copper minerals encountered in the sulphide deposits are represented by covellite, malachite, chrysocolla and atacamite.

Covellite is characterized by blue color, with strong pleochrism ranging from dark blue to blue. The mineral has moderate reflectivity and distinct anisotropic.

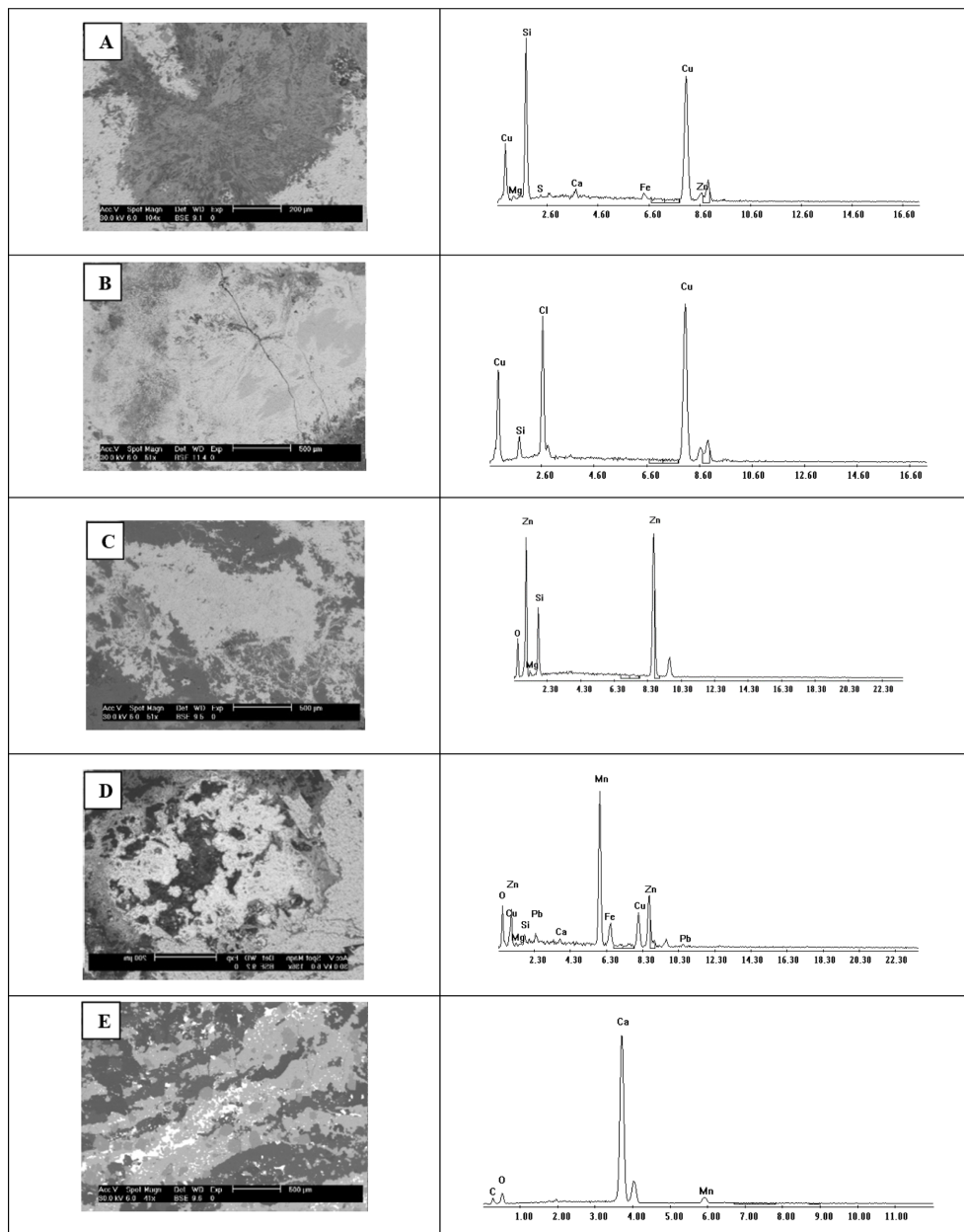


*Fig. 3.* SEM image and EDX analysis data of A) Chrysocolla, B) Atacamite, C) Calamine, D) Bixbyite and E) Calcite minerals.

Covellite is commonly found in small patches because of alteration of chalcopyrite. Malachite ( $\text{CuCO}_3(\text{OH})_2$ ) occurs as pseudomorphs after chalcopyrite in the oxidized zone of copper deposits. It is cryptocrystalline mineral filling fracture.

Chrysocolla ( $\text{CuSiO}_3 \cdot n\text{H}_2\text{O}$ ) is present as anhedral aggregates commonly pseudomorphs after malachite as shown in *Fig. 3A*. Atacamite ( $\text{CuCl}_2 \cdot 3\text{Cu}(\text{OH})_2$ ) is detected as minute anhedral aggregate found close or nearby other ore minerals as shown in *Fig. 3B*. Calamine ( $\text{Zn}_4\text{Si}_2\text{O}_7(\text{OH})_2 \cdot \text{H}_2\text{O}$ ) is present as anhedral aggregates commonly pseudomorphous after zinc minerals. It forms in the zone of oxidation in the course of weathering of lead-zinc sulphide deposits as shown in *Fig. 3C*.

Bixbyte ( $(\text{Mn,Fe})_2\text{O}_2$ ) is secondary iron-manganese mineral formed in the oxidizing zone of sulphide deposits. It is occurring as anhedral aggregates embedded in the carbonate and quartz minerals as shown in *Fig. 3D*. Carbonates are mainly Calcite, have been detected as the main abundant gangue minerals, filling the interstitial spaces between the sulphide minerals as shown in *Fig. 3E*. Occasionally, it is found in the form of microveinlets filling fractures with quartz. Quartz occurs as colorless anhedral crystals showing undulose extinction. Talc occurs as independent minute flakes associated with carbonate minerals.

In conclusion, the sulfide mineralization consists mainly of chalcopyrite, sphalerite, pyrite, galena and bornite arranged in a decreasing order of abundance. Silver is detected only by SEM as rare, disseminated crystals within the gangue minerals. Under supergene conditions, secondary copper minerals (covellite, malachite, chrysocolla and atacamite) were formed. Secondary zinc mineral was formed in this stage and represented by calamine. Secondary iron-manganese mineral was formed because of the replacement process of pyrite and chalcopyrite. On the other side, the gangue minerals are represented by quartz, carbonate minerals (calcite), talc and opaques.

### 3.1.2. Chemical investigation

It is well known that the nature and mode of

Table 1. Major elemental analysis of the sulphide deposit from Abu Gurdi area

Component	wt. %
$\text{SiO}_2$	6.12
$\text{TiO}_2$	0.04
$\text{Al}_2\text{O}_3$	5.89
$\text{Fe}_2\text{O}_3$	15.24
CaO	32.45
$\text{K}_2\text{O}$	0.34
$\text{P}_2\text{O}_5$	0.90
$\text{Na}_2\text{O}$	0.90
L.O.I.	33.97

occurrence of mineralization and its associated gangues control the rate of dissolution and recoveries of the incorporated metals of interest. The chemical composition of the studied Abu Gurdi area is presented in *Table 1*.

It is clear that, the considered sample is composed mainly of CaO and  $\text{Fe}_2\text{O}_3$  of 32.45 % and 15.24 %, respectively and low  $\text{SiO}_2$  of 6.12 %. These oxides are chiefly occurred as calcium carbonate and oxides minerals beside hematite and goethite. Concerning the economic metal values, the used ore contains 1.2 %, 0.66 % and 0.95 % of Zn, Cu and Pb, respectively as shown in *Table 2*, which reflects the importance of their recovery from the considered ore.

The mineralogical and chemical composition of the considered sulfide deposits from Abu Gurdi area, enhancing the application of alkaline leaching process

Table 2. Chemical analysis of trace elements of the sulfide deposits from Abu Gurdi area

Element	%
Fe	4.762
U	0.31812
Pb	0.9538
Ce	0.33035
Cu	0.6589
Sr	0.036
Rb	0.003
Zn	1.188
Mn	1.770
Ti	0.035
Ca	0.156
Au	0.0004

for the extraction of high purity metal ions using cost-effective technologies.

### 3.2. Optimization the leaching process

Factors affecting the dissolution efficiencies of the Zn, Cu and Pb metals ions have been investigated to optimize the leaching process. It has been noted that alkaline leaching can be more effective for certain sulfide deposits of Abu Gurdy area with large amounts of acid-consuming carbonate rocks, as the leaching process is much more selective.<sup>54</sup>

#### 3.2.1. Effect of reagent composition

In order to enhance the leaching process for Zn, Cu and Pb, many reagent types have been investigated to select the more effective reagent. The effect of reagent composition on the efficiency of the leaching process was carried out using different alkali reagents such as  $\text{NH}_4\text{OH}$ ,  $\text{Na}_2\text{CO}_3 - \text{NaHCO}_3$  mixture,  $(\text{NH}_4)_2\text{CO}_3 - \text{NH}_4\text{HCO}_3$  mixture,  $(\text{NH}_4)\text{HCO}_3$  and  $\text{Na}_2\text{CO}_3 - (\text{NH}_4)\text{HCO}_3$  mixture at total alkali concentration of 250 g/L. All the leaching experiments were carried out at a constant leaching condition of 150 °C for 3h and at 1/3 S/L ratio and the obtained results are presented in Fig. 4.

The obtained results showed that the leaching reagent consisting of  $\text{Na}_2\text{CO}_3 - \text{NaHCO}_3$  mixture has the greatest effect upon the leachability of all metal ions of interest which are 84.09 %, 74.89 % and 64.69 % for Zn, Cu and Pb, respectively. On the other hand, using  $\text{NH}_4\text{OH}$  as leaching reagent showed the lowest effect upon the leachability of all metal ions of interest which are 24.11 %, 11.28 % and 8.90 % for Zn,

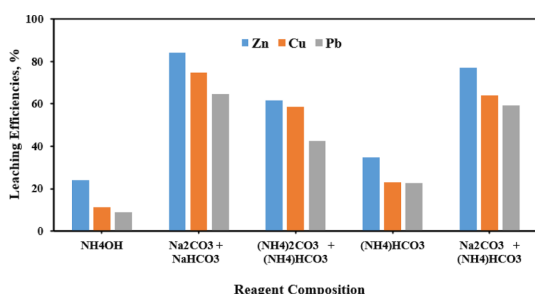


Fig. 4. Effect of reagent composition upon leaching efficiencies of Zn, Cu and Pb metal ions.

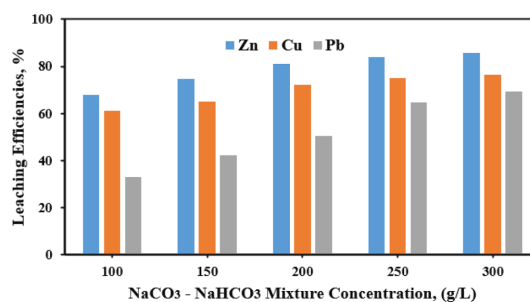


Fig. 5. Effect of  $\text{Na}_2\text{CO}_3 - \text{NaHCO}_3$  mixture concentration upon leaching efficiencies of Zn, Cu and Pb metal ions.

Cu and Pb, respectively. The leaching reagent can be ordered according to effectiveness from the lower to the higher as follow;  $\text{NH}_4\text{OH}$ ,  $(\text{NH}_4)\text{HCO}_3$ ,  $(\text{NH}_4)_2\text{CO}_3 - (\text{NH}_4)\text{HCO}_3$  mixture,  $\text{Na}_2\text{CO}_3 - (\text{NH}_4)\text{HCO}_3$  mixture and  $\text{Na}_2\text{CO}_3 - \text{NaHCO}_3$  mixture.

#### 3.2.2. Effect of $\text{Na}_2\text{CO}_3 - \text{NaHCO}_3$ mixture concentration

The Effect of  $\text{Na}_2\text{CO}_3 - \text{NaHCO}_3$  mixture concentration on the leaching efficiencies of Zn, Cu and Pb metal ions was studied using different total alkali concentrations of  $\text{Na}_2\text{CO}_3 - \text{NaHCO}_3$  mixture ranging from 100 to 300 g/L at a mixing ratio of 3/1. The other leaching conditions were fixed at 150 °C for 3h and at 1/3 S/L ratio. The obtained results presented in Fig. 5 showed that the leaching efficiencies of all the interesting elements continuously increase with increasing the reagent solution concentration from 100 to 300 g/L. The percent recovery of Zn increases from 69.1 to 84.1 %, Cu from 61.04 to 74.6 % and Pb from 33.1 % to 64.9 % at alkali concentration of 250 g/L. Increasing the alkali concentration of  $\text{Na}_2\text{CO}_3 - \text{NaHCO}_3$  mixture concentration to 300 g/L has a slight influence upon the leaching efficiency of all elements.

#### 3.2.3. Effect of leaching time

The effect of leaching time upon the leaching efficiencies of Zn, Cu and Pb were investigated by varying the leaching time from 1 to 5 hr. at 1 hr. step and the other leaching parameter were remained constant at 250 g/L  $\text{Na}_2\text{CO}_3 - \text{NaHCO}_3$  alkali concen-

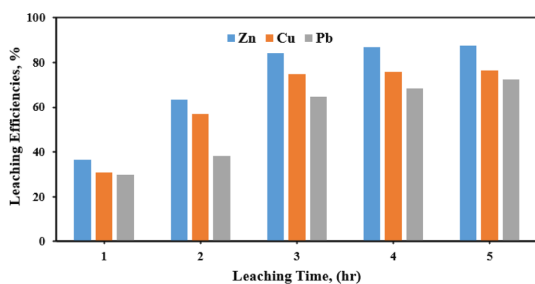


Fig. 6. Effect of leaching time upon leaching efficiencies of Zn, Cu and Pb metal ions.

tration, 1/3 S/L ratio and at 150 °C and the obtained results are presented in Fig. 6. It is clear that the percent recoveries of Zn, Cu, Pb are increased gradually with increasing the leaching time from 1 to 3 hr. The percent recoveries of Zn, Cu, Pb increases from 36.55 %, 30.76 %, 29.67 %, respectively to 84.09 %, 74.89 %, 64.69 %, respectively. It is shown that increasing the leaching time more than 3 hr. has a slight effect on the percent recoveries of all the elements of interest, so that the leaching time of 3 hr. was selected as the best leaching time.

#### 3.2.4. Effect of leaching temperature

The effect of leaching temperature upon the leaching efficiencies of Zn, Cu and Pb were investigated by varying the leaching temperature from 50 °C to 250 °C at 50 °C step and the other leaching parameter were remained constant at 250 g/l NaCO<sub>3</sub> - NaHCO<sub>3</sub> alkali concentration, 1/3 S/L ratio and at 3 hr. leaching time and the obtained results are presented in Fig. 7. It is clear that the percent recoveries of Zn, Cu and Pb are increased gradually with increasing the leaching tem-

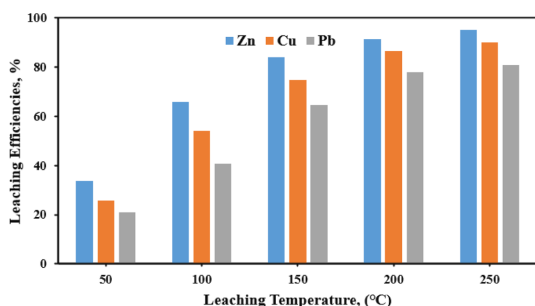


Fig. 7. Effect of leaching temperature upon leaching efficiencies of Zn, Cu and Pb metal ions.

perature from 50 °C to 250 °C. The percent recoveries of Zn, Cu and Pb increases from 33.78 %, 25.67 % and 20.90 %, respectively to 95.11 %, 90.23 % and 80.78 %, respectively. Due to the difficulty of using high temperature and unavailability of the appropriate equipment for this, so that the leaching temperature of 250 °C was selected as the best leaching temperature.

#### 3.2.5. Effect of solid/liquid ratio (W/V)

The effect of solid / liquid ratio upon the leaching efficiencies of Zn, Cu and Pb were investigated by varying the S/L ratio from 1/2 to 1/5 and the other leaching parameter were remained constant at 250 g/l NaCO<sub>3</sub> - NaHCO<sub>3</sub> alkali concentration, 3 hr. leaching time and 250 °C leaching temperature and the obtained results are presented in Fig. 8. It is clear that the percent recoveries of Zn, Cu and Pb are increasing gradually with increasing the S/L ratio from 1/2 to 1/5. The percent recoveries of Zn, Cu and Pb increases from 79.53 %, 76.88 % and 66.78 %, respectively to 99.48 %, 96.70 % and 99.11 %, respectively. Increasing the S/L ratio from 1/2 to 1/5 increases the leaching efficiencies of the metal ions of interest due to increasing the amount of leaching solution which contains high amount of reagent ions which increases the possibility of leaching process, and the solid particles are well exposed to the liquid molecules. So that the solid / liquid ratio of 1/5 was recommended to be the best to obtain the maximum percent recoveries of all the metal ions of interest.

From the previous study, for obtaining the maximum recovery of all elements of interest (Zn, Cu, and Pb),

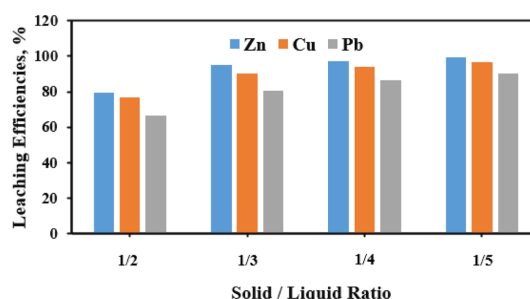


Fig. 8. Effect of solid/liquid ratio upon leaching efficiencies of Zn, Cu and Pb metal ions.

the recommended leaching conditions are as follow; 250 g/L  $\text{NaCO}_3$  -  $\text{NaHCO}_3$  alkali concentration, 3 hr. leaching time, 250 °C leaching temperature, and 1/5 solid : liquid ratio.

### 3.3. Kinetics of leaching process

Conventionally, the kinetics of chemical reactions involving solids and fluids have been modeled using the un-reacted shrinking core models. It is the most commonly used mathematical model to describe heterogeneous reactions like mineral leaching from ores.<sup>55</sup> The model assumes that an ash layer is formed around a shrinking core of unreacted solid reactant during the reaction. It is well known that three possible resistances will control the reaction: 1) diffusion through the fluid film surrounding the particle, 2) the chemical reaction itself, 3) or diffusion through the ash layer of the product. Depending on the reaction occurring, one or a mixture of the resistances mentioned above can occur to develop a model that will predict how that particular chemical process will proceed with time.<sup>56</sup> The simplified equations of the shrinking core model can be expressed as follows:<sup>57</sup> When

diffusion through the fluid film controls, this process modeled as:

$$K_1 t = 1 - (1 - \alpha) \quad (1)$$

When the chemical reaction controls, the process can be modeled as:

$$K_2 t = 1 - (1 - \alpha)^{1/3} \quad (2)$$

When diffusion process through the solid controls, this reaction modeled as:

$$K_3 t = 1 - 3(1 - \alpha)^{2/3} + 2(1 - \alpha) \quad (3)$$

Where  $\alpha$  is the fractional conversion of the solid, when both the chemical control reaction and diffusion reaction through the fluid film controls, the overall resistance can be taken as the sum of the two individual resistances since the resistances occur in series and hence can be expected to be additive,<sup>57</sup>  $K$  is the apparent rate constant and it is the slope of the line while  $t$  is the time of reaction.

The two shrinking core models following the Eqs. (2) and (3) could be examined at different temperatures for the elements of interest (Zn, Cu and Pb) as

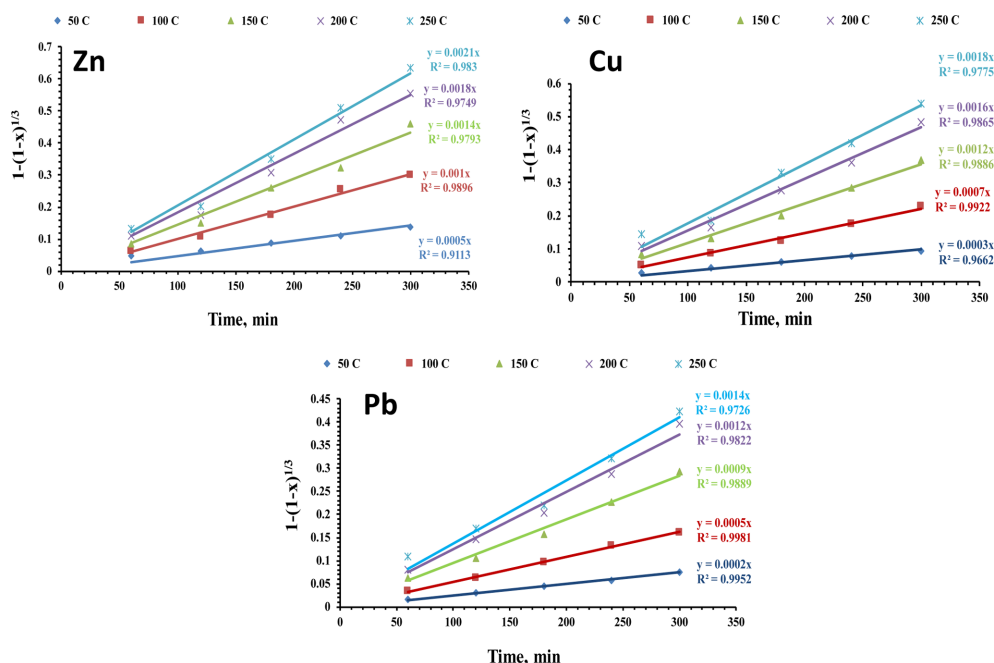


Fig. 9. Effect of dissolution time upon leaching efficiencies of Zn, Cu and Pb at various temperatures using the function  $[1 - (1 - \alpha)^{1/3}]$ .

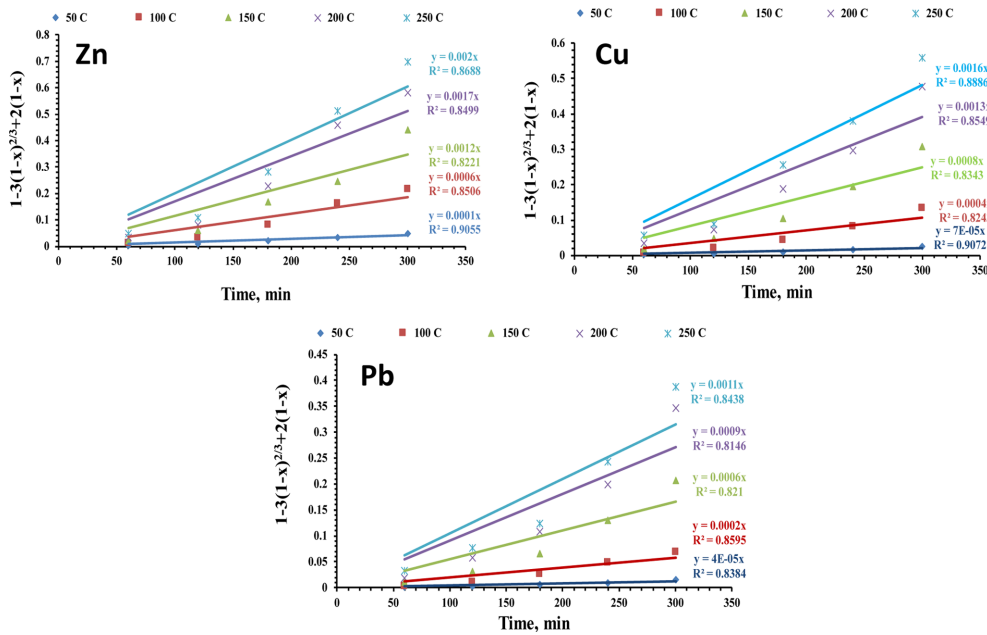


Fig. 10. Effect of dissolution time upon leaching efficiencies of Zn, Cu and Pb at various temperatures using the function  $[1 - 3(1 - \alpha)^{2/3} + 2(1 - \alpha)]$ .

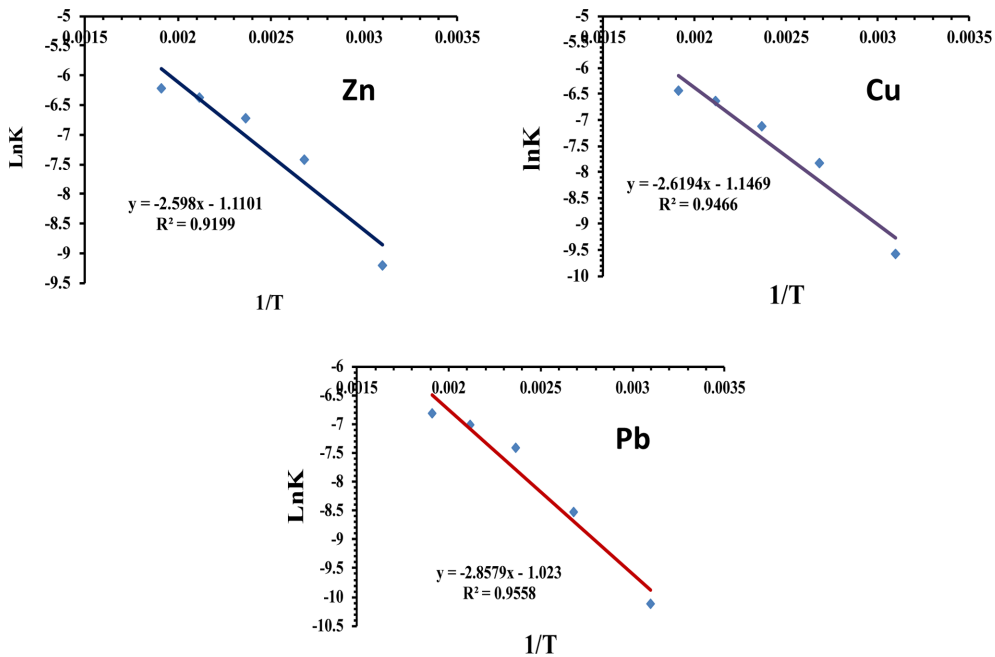


Fig. 11. Activation energy calculation of interesting elements from the Arrhenius plot.

illustrated in Figs. 9 and 10. These figures show that only Eq. (2) has been found to give an acceptable straight line for all the elements of interest with an average correlation of 0.983, 0.899, and 0.973,

respectively. The resulting slopes of each line in Fig. 11 were calculated and demonstrated the apparent reaction rate constants  $K_2$ . The activation energy under the effect of different temperature was evaluated for

each studied element, where the Arrhenius equation can express the relation between the rate constant,  $K_2$ , obtained at different temperatures:  $K = A$

Where  $K$  is the overall rate constant in  $\text{min}^{-1}$ ,  $A$  is the frequency factor in  $\text{min}^{-1}$ ,  $E_a$  is the activation energy in  $\text{J mol}^{-1}$ ,  $R$  is the universal gas constant ( $8.314 \text{ J K}^{-1} \text{ mol}^{-1}$ ), and  $T$  is the reaction temperature in  $^\circ\text{K}$ .

Displaying the natural logarithmic values of dissolution rate constants ( $\ln K$ ) of Zn, Cu and Pb in dissolution process as a function in ( $1/T$ ) is presented in *Fig. 11*. According to the Arrhenius equation, the obtained activation energy of the dissolution reaction of Zn, Cu and Pb from Abu Gurdi area massive sulfide by  $\text{Na}_2\text{CO}_3$  -  $\text{NaHCO}_3$  mixture equals 21.599, 21.779 and 23.761  $\text{Kj}\cdot\text{mol}^{-1}$ , respectively. The diffusion-controlled process has an activation energy of around  $< 12 \text{ kJ}\cdot\text{mol}^{-1}$ , while the chemical reaction-controlled process often has an activation energy of  $> 40 \text{ kJ}\cdot\text{mol}^{-1}$ ; when activation energy is between 12 and 40  $\text{kJ}\cdot\text{mol}^{-1}$ , the process is controlled by both diffusion and chemical reaction.<sup>58</sup>

The current study shows that the apparent activation energy was between those of a typical diffusion-controlled process and a chemical reaction-controlled process, providing more evidence to prove that the  $\text{Na}_2\text{CO}_3$ - $\text{NaHCO}_3$  mixture leaching process was controlled by both internal diffusion and interface chemical reactions.<sup>56</sup> This can be attributed to the alkaline concentration decreasing as the leaching process proceeded. Thus, the chemical reaction rate decreased, resulting in the chemical reaction becoming part of the rate-controlling step.

Since the calculated value of 21.599, 21.779 and 23.761  $\text{kJ}\cdot\text{mol}^{-1}$  for Zn, Cu and Pb, respectively are near the value of 12  $\text{kJ}\cdot\text{mol}^{-1}$  significantly, the diffusion of the solid product layer contributed more than the chemical reaction to control the rate of the leaching process.<sup>59</sup>

### 3.4. The separation on individual metal ions

#### 3.4.1. preparation of carbonate pregnant solution

One kg of working of Abu Gurdi ore sample has undergone an alkaline leaching process under the previously optimized leaching conditions (250 g/L

$\text{NaCO}_3$  -  $\text{NaHCO}_3$  reagent concentration, 3 hr., 250  $^\circ\text{C}$  and 1/5 S/L ratio). The obtained leach liquor is then treated to recover separated metal ions Zn, Cu and Pb from the carbonate solution. The obtained leaching liquor of 5000 ml has been analyzed for Zn, Cu and Pb using the former test, which indicate that it contains 2.36, 1.27, and 1.7 g/L, respectively, with leaching efficiency of 99.5 %, 96.7 % and 90.1 %, respectively.

#### 3.4.2. Recovery of interesting elements from prepared carbonate solution

In order to obtain individual metal ions from leach liquor, the procedure presented in *Fig. 12* was applied.

Firstly, the leach liquor was adjusted by adding NaOH to convert the metal ions into the hydroxide forms as a bulk hydroxide by adjusting pH at 7. Then, the three metal ions were dissolved into sulfuric acid by heating. Firstly, pure copper was separated by adjusting the pH at 5.3-5.5. The copper was

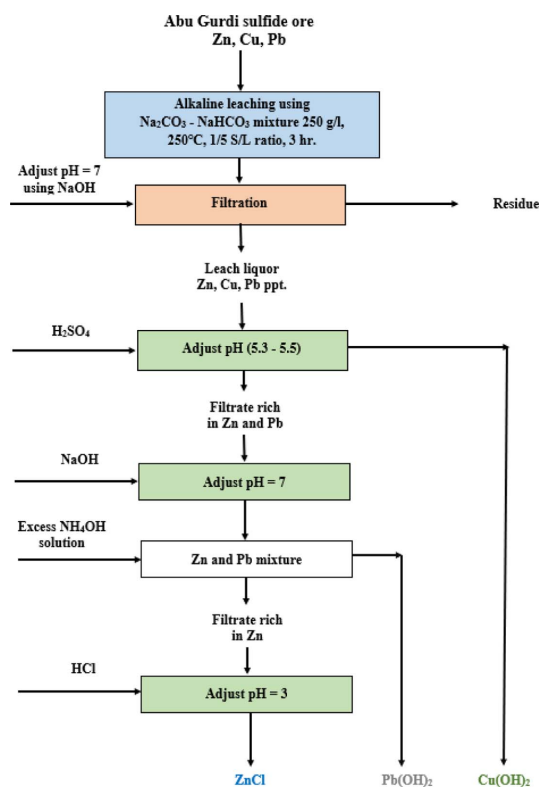


*Fig. 12.* The proposed flow sheet for processing Abu Gurdi ore sample for the extraction of  $\text{Cu(OH)}_2$ ,  $\text{Pb(OH)}_2$ , and  $\text{ZnCl}_2$ .

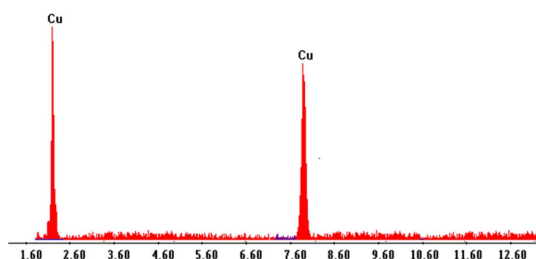


Fig. 13. EDX-analysis of the precipitated  $\text{Cu}(\text{OH})_2$ .

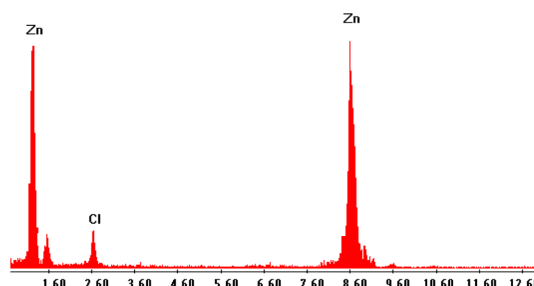


Fig. 15. EDX-analysis of the precipitated  $\text{ZnCl}_2$ .

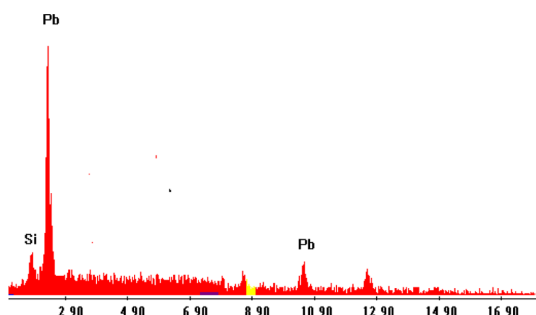


Fig. 14. EDX-analysis of the precipitated  $\text{Pb}(\text{OH})_2$ .

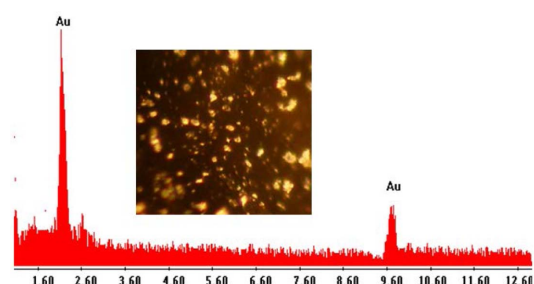


Fig. 16. EDX-analysis of the obtained Au metal from Abu Gurdi ore sample.

precipitated as  $\text{Cu}(\text{OH})_2$  as shown in Fig. 13.

Pb and Zinc were lifted behind dissolved in the solution. In order to separate Pb from the solution containing Pb and Zn metal ions, the solution pH was first adjusted at pH 7 by adding NaOH. Then, excess of ammonia solution was added to the Pb-Zn leach liquor solution to dissolve the zinc metal ions in the excess of ammonia solution white lead (II) hydroxide  $\text{Pb}(\text{OH})_2$  was precipitate. The EDX analysis of obtained  $\text{Pb}(\text{OH})_2$  is shown in Fig. 14. Then, Zn was precipitated as  $(\text{ZnCl})$  from the remaining solution by adjusting pH = 3 using HCl solution. The EDX-analysis of the obtained  $\text{ZnCl}$  is shown in Fig. 15.

#### 3.4.3. Recovery of gold from raw material

According to<sup>60</sup> and using the studied optimum conditions of Au adsorption from the working technological ore sample (4ppm Au); namely 120 g/L  $\text{H}_2\text{SO}_4$  acid concentration, -60 mesh size of ore with 1/5 solid/liquid and for 20 min. An adsorption experiment was made using 500 g of the ore sample, however non-enriched with any commercial Au. The obtained result revealed that 0.3 g in-situ formed calcium sulfate scales in the meantime, the ascending gold

particles were found to be surface adsorbed the in-situ formed  $\text{CaSO}_4$ . Then, native Au particles from the working sample were collected. Calcium sulfate was washed with a large amount of water up to 2 liters through the filter paper to leave behind the Au particles of 100 % purity was revealed. EDX-analysis of the obtained Au is presented in Fig. 16.

## 4. Conclusions

The obtained results of mineralogical study indicate the existence of huge assemblages of valuable minerals mainly represented by Zn, Cu and Pb minerals. On the other hand, leaching studies of Abu Gurdi volcanic massive sulphide deposits (VMS) sample was investigated by mixture of  $\text{Na}_2\text{CO}_3 + \text{NaHCO}_3$  using agitation leaching process. The maximum dissolution efficiencies of Cu, Zn, and Pb at the optimum leaching conditions i.e., 250 g/L  $\text{NaCO}_3 - \text{NaHCO}_3$  alkali concentration, for 3 hr., at 250 °C, and 1/5 S/L ratio., were 99.48 %, 96.70 % and 99.11 %, respectively. An apparent activation energy for Zn, Cu and Pb dissolution were 21.599, 21.779 and

23.761 kJ.mol<sup>-1</sup>, respectively, which were between those of a typical diffusion-controlled process and a chemical reaction-controlled process. Bulk hydroxide precipitation technique was applied at pH 7 for precipitating Zn, Cu and Pb hydroxide cake. The latter subjected to complete dissolution in H<sub>2</sub>SO<sub>4</sub> acid followed by individual precipitation of each element. High pure Cu(OH)<sub>2</sub>, Pb(OH)<sub>2</sub>, and ZnCl<sub>2</sub> were obtained from the finally obtained leach liquor at the optimum leaching conditions by precipitation at different pH. Finally, highly pure Au metal was separated from the mineralized massive sulfide via using adsorption method.

### Acknowledgements

The authors are also thankful to Prof. Dr. Enass Mohamed El-Sheikh, Nuclear Materials Authority, Maadi, Cairo, Egypt for his valuable feedback on the first draft.

### References

1. P. A. Olubambi, J. O. Borode, and S. Ndlovu, *The Journal of The Southern African Institute of Mining and Metallurgy*, **106** (11), 765-770 (2006). [https://hdl.handle.net/10520/AJA0038223X\\_3209](https://hdl.handle.net/10520/AJA0038223X_3209)
2. A. Potysz, E. D. Van Hullebusch, J. Kierczak, M. Grybos, P. N. L. Lens, and G. Guibaud, *Rev. Environ. Sci. Technol.*, **45**(22), 2424-2488 (2015). <https://doi.org/10.1080/10643389.2015.1046769>
3. P. Sarfo, A. Das, G. Wyss, and C. Young, *Waste Manag.*, **70**, 272-281 (2017). <https://doi.org/10.1016/j.wasman.2017.09.024>
4. K. S. Barros, V. S. Vielmo, B. G. Moreno, G. Riveros, G. Cifuentes, and A. M. Bernardes, *Minerals*, **12**, 250 (2022). <https://doi.org/10.3390/min12020250>
5. S. S. Jena, S. K. Tripathy, N. R. Mandre, R. Venugopal, and S. Farrokhpay, *Minerals*, **12**, 545 (2022). <https://doi.org/10.3390/min12050545>
6. J. Lee, S. Kim, B. Kim, and J. C. Lee, *Metals*, **8**(3), 150 (2018). <https://doi.org/10.3390/met8030150>
7. M. Sokic, B. Markovic, S. Stankovic, Ž. Kamberovic, N. Štrbac, V. Manojlovic, and N. Petronijevic, *Metals*, **9**, 1173 (2020). <https://doi.org/10.3390/met9111173>
8. J. Dutrizac, *Hydrometallurgy*, **29**(1-3), 1-45 (1992). [https://doi.org/10.1016/0304-386X\(92\)90004-J](https://doi.org/10.1016/0304-386X(92)90004-J)
9. R. P. Hackl, D. B. Dreisinger, E. Peters, and J. A. King, *Hydrometallurgy*, **39**(1-3), 25-48 (1995). [https://doi.org/10.1016/0304-386X\(95\)00023-A](https://doi.org/10.1016/0304-386X(95)00023-A)
10. Z. Lu, M. Jeffrey, and F. Lawson, *Hydrometallurgy*, **56**(2), 189-202 (2000). [https://doi.org/10.1016/S0304386X\(00\)00075-X](https://doi.org/10.1016/S0304386X(00)00075-X)
11. F. Carranza, N. Iglesias, A. Mazuelos, I. Palencia, and R. Romero, *Hydrometallurgy*, **71**(3-4), 413-420 (2004). [https://doi.org/10.1016/S0304386X\(03\)00119-1](https://doi.org/10.1016/S0304386X(03)00119-1)
12. P. C. Hernández, J. Dupont, O. O. Herreros, Y. P. Jimenez, and C. M. Torres, *Minerals*, **9**(4), 250 (2019). <https://doi.org/10.3390/min9040250>
13. N. Sabba and D.E. Akretche, *Minerals Engineering*, **19**(12), 123-129 (2006). <https://doi.org/10.1016/j.mineng.2005.08.015>
14. J. O. Marsden, J. C. Wilmot, and N. Hazen, *Mining, Metallurgy & Exploration*, **24**, 193-204 (2007). <https://doi.org/10.1007/BF03403368>
15. D. D. Wu, S. M. Wen, J. S. Deng, and J. Liu, *Journal of Chemical Engineering of Japan*, **46**, 677-682 (2013). <https://doi.org/10.1252/jcej.13we035>
16. A. Grizo, N. Pacović, F. Poposka, and Ž. Koneska, *Hydrometallurgy*, **8**(1), 5-16 (1982). [https://doi.org/10.1016/0304-386X\(82\)90026-3](https://doi.org/10.1016/0304-386X(82)90026-3)
17. D. Bingöl and M. Canbazoğlu, *Hydrometallurgy*, **72**(1-2), 159-165 (2004). <https://doi.org/10.1016/j.hydromet.2003.10.002>
18. N. Habbache, N. Alane, S. Djerad, and L. Tifouti, *Chemical Engineering Journal*, **152**, 503-508 (2009). <https://doi.org/10.1016/j.cej.2009.05.020>
19. H. Razavizadeh and M. R. Afshar, *Mining, Metallurgy & Exploration*, **25**, 85-90 (2008). <https://doi.org/10.1007/BF03403391>
20. K. Xiong, S. M. Wen, G. S. Zheng, S. J. Bai, and H. Y. Shen, *Advanced Materials Research*, **524-527**, 987-992 (2012). <https://doi.org/10.4028/www.scientific.net/amr.524-527.987>
21. O. Levenspiel, *Chemical Reaction Engineering: An introduction to the design of chemical reactors*. 1<sup>st</sup> ed., John Wiley & Sons: New York, 17-26, 343-350 (1962).
22. H. S. Fogler, *Elements of Chemical Reaction Engineering*.

- Prentice-Hall International Inc.: New Jersey, USA, 1986.
23. M. Coulson, J. F. Richardson, Chemical Engineering. Pergamon Press: Oxford, **1**, 268-269, 343 (1977).
  24. R. Z. Vracar, N. Vuckovic, and Z. Kamberovic, *Hydrometallurgy*, **70**(1-3), 143-151 (2003). [https://doi.org/10.1016/S0304-386X\(03\)00075-6](https://doi.org/10.1016/S0304-386X(03)00075-6)
  25. R. J. Stem, A. Kröner, W. I. Manton, T. Reischmann, M. Mansour, and I. M. Hussein, *Journal of the Geological Society London*, **146**, 1017-1029 (1989).
  26. A. Kröner, W. Todt, I. M. Hussein, M. Mansour, and A. A. Rashwan, *Precambrian Research*, **59**(1-2), 15-32 (1992). [https://doi.org/10.1016/0301-9268\(92\)90049-T](https://doi.org/10.1016/0301-9268(92)90049-T)
  27. A. Fowler and B. El Kalioubi, *Journal of African Earth Sciences*, **38**(1), 23-40 (2004). <https://doi.org/10.1016/j.jafrearsci.2003.09.003>
  28. M. W. Ali-Bik, M. F. Sadek, and D. Sadek Ghabrial, *Journal of African Earth Sciences*, **99**, 24-38 (2014). <https://doi.org/10.1016/j.jafrearsci.2013.08.010>
  29. P. R. Johnson, *The Open Geology Journal*, **8**, 3-33 (2014). <https://doi.org/10.2174/1874262901408010003>
  30. M. K. Jha, V. Kumar, and R. J. Singh, *Resour. Conserv. Recy.*, **33**(1), 1-22 (2001). [https://doi.org/10.1016/S0921-3449\(00\)00095-1](https://doi.org/10.1016/S0921-3449(00)00095-1)
  31. EGSM (Egyptian Geological Survey and Mining Authority), Geologic map of Al Qusayr Quadrangle, Egypt. Egyptian Geological Survey, Cairo. 1992.
  32. E. A. Abdel-Aal, *Hydrometallurgy*, **55**(3), 247-254 (2000). [https://doi.org/10.1016/S0304-386X\(00\)00059-1](https://doi.org/10.1016/S0304-386X(00)00059-1)
  33. S. Ju, T. Motang, Y. Shendhai, and L. Yingian, *Hydrometallurgy*, **80**(1-2), 67-74 (2005). <https://doi.org/10.1016/j.hydromet.2005.07.003>
  34. S. Espiari, F. Rashchi, and S. K. Sadmezzaad, *Hydrometallurgy*, **82**(1-2), 54-62 (2006). <https://doi.org/10.1016/j.hydromet.2006.01.005>
  35. Rx. Wang, Mt. Tang, Sh. Yang, Wh. Zhagn, Cb. Tang, J. He, and J. Yang, *J. Cent. South Univ. Technol.*, **15**, 679-683 (2008). <https://doi.org/10.1007/s11771-008-0126-4>
  36. M. Hursit, O. Lacin, and H. Sarac, *J. Taiwan Inst. Chem. Eng.*, **40**(1), 6-12 (2009). <https://doi.org/10.1016/j.jtice.2008.07.003>
  37. R. Larba, I. Boukerche, N. Alane, N. Habbache, S. Djerad, and L. Tifout, *Hydrometallurgy*, **134-135**, 117-123 (2013). <https://doi.org/10.1016/j.hydromet.2013.02.002>
  38. M. Irannajad, M. Meshkini, and A. Azadmehr, *Physicochem. Probl. Miner. Process*, **49**(2), 547-555 (2013). <https://doi.org/10.5277/ppmp130215>
  39. D. D. Wu, S. M. Wen, J. Yang, and J. S. Deng, *Canadian Metallurgical Quarterly*, **54**(1), 51-57 (2015). <https://doi.org/10.1179/1879139514Y.0000000150>
  40. A. B. ElDeeb, V. N. Brichkin, R. V. Kurtenkov, and I.S. Bormotov, *Obogashchenie Rud*, **2**, 27-32 (2021). <https://www.rudmet.ru/journal/2004/article/33690/?language=en>
  41. A. B. ElDeeb, V. N. Brichkin, M. Bertau, M. E. Awad, and Y. A. Savinova, *Clay Minerals*, **56**(4), 269-283 (2022). <https://doi.org/10.1180/clm.2022.7>
  42. A. B. ElDeeb, V. N. Brichkin, V. G. Povarov, and R. V. Kurtenkov, *Tsvetnye Metally*, **7**, 18-25 (2020). <https://www.rudmet.ru/journal/1936/article/32742/?language=en>
  43. A. Chen, Z.W. Zhao, X. Jia, S. Long, G. Huo, and X. Chen, *Hydrometallurgy*, **97**(3-4), 228-232 (2009). <https://doi.org/10.1016/j.hydromet.2009.01.005>
  44. F. M. F. Santos, P. S. Peina, A. Porcaro, V. A. Oliviera, C. A. Silva, and V. A. Leão, *Hydrometallurgy*, **102**(1-4), 43-49 (2010). <https://doi.org/10.1016/j.hydromet.2010.01.010>
  45. Y. Zhang, J. Deng, J. Chen, R. Yu, and X. Xing, *Hydrometallurgy*, **131-132**, 89-92 (2013). <https://doi.org/10.1016/j.hydromet.2012.10.007>
  46. S. Nagib and K. Inoue, *Hydrometallurgy*, **56**(3), 269-292 (2000). [https://doi.org/10.1016/S0304-386X\(00\)00073-6](https://doi.org/10.1016/S0304-386X(00)00073-6)
  47. D. K. Xia and C. A. Pickles, *Minerals Engineering*, **13**(1), 79-94 (2000). <https://doi.org/10.1016/j.mineng.2005.08.013>
  48. Y. Zhao and R. Stanforth, *Hydrometallurgy*, **56**(2), 237-249 (2000). [https://doi.org/10.1016/S0304-386X\(00\)00079-7](https://doi.org/10.1016/S0304-386X(00)00079-7)
  49. C. Jarupisitthorn, T. Pimtong, and G. Lothongkum, *Mater. Chem. Phys.*, **77**(2), 531-535 (2003). [https://doi.org/10.1016/S0254-0584\(02\)00119-0](https://doi.org/10.1016/S0254-0584(02)00119-0)
  50. M. Erdem and M. Yurten, *Journal of Mining and Metallurgy, Section B: Metallurgy*, **51**(1), 89-95 (2015). <http://dx.doi.org/10.2298/JMMB140503012E>
  51. S. M. S. Ghasemi and A. Azizi, *J. Mater. Res. Technol.*, **7**(2), 118-125 (2018). <http://dx.doi.org/10.1016/j.jmrt.2017.03.005>
  52. N.W. Burger, *Amer. Mineral*, **19**(11), 525-530 (1934).
  53. G. M. Schwartz, *Econ. Geol.*, **26**, 186 (1931).
  54. F. Parada, M. I. Jeffrey, and E. Asselin, *Hydrometallurgy*, **146**, 48-58 (2014). <https://doi.org/10.1016/j.hydromet.2014.03.003>
  55. A. H. Ibrahim, X. Lyu, and A. B. ElDeeb, *Nanomaterials*,

- 13(6), 1091 (2023). <https://doi.org/10.3390/nano13061091>
56. A. H. Ibrahim, X. Lyu, B.M. Atia, M. A. Gado, and A. B. ElDeeb, *Journal of Material Cycles and Waste Management*, **25**(1), 86-102 (2023). <https://doi.org/10.1007/s10163-022-01512-8>
57. G. M. A. Mahran, M. A. Gado, W. M. Fathy, and A. B. ElDeeb, *Materials*, **16**(13), 4662 (2023). <https://doi.org/10.3390/ma16134662>
58. M. Ashraf, Z. I. Zafar, and T. M. Ansari, *Hydrometallurgy*, **80**(4), 286-292 (2005). <https://doi.org/10.1016/j.hydromet.2005.09.001>
59. A. H. Ibrahim, X. Lyu, B. M. Atia, M. A. Gado, and A. B. ElDeeb, *Minerals*, **12**, 1084 (2022). <https://doi.org/10.3390/min12091084>
60. R. Sousa, M. J. Regufe, A. Fiúza, M. M. Leite, and A. Futuro, *The Extractive Industries and Society*, **9**, 101018 (2022). <https://doi.org/10.1016/j.exis.2021.101018>

---

### Authors' Positions

Ibrahim A. Salem : Professor  
Gaafar A. El Bahariya : Professor  
Bothina T. El Dosuky : Professor  
Eman F. Refaey : Demonstrator  
Ahmed H. Ibrahim : Lecturer  
Amr B. ElDeeb : Lecturer